OPTIMUM DESIGN OF COMPOSITE PRIMARY STRUCTURE AIRCRAFT COMPONENTS

by

D. M. Purdy
Branch Chief – Design
Structural Advanced Technology

and

C. G. Dietz
Senior Engineer/Scientist
Structural Advanced Technology

Douglas Aircraft Company
McDonnell Douglas Corporation
Long Beach, California

ABSTRACT

The application of advanced composite materials to aircraft structures holds the potential for significant improvements in the aircraft system. The application of these materials in primary structures is evaluated and a methodology discussed for determining the optimum configurations of the primary structure components. The procedure goes beyond establishing optimum laminate patterns and determines the appropriate size, shape, and spacing of any stiffener materials. Constraints which may be applied to the optimization process include manufacturing, strain, and stiffness requirements. The impact on the structural weight of various potential constraints is examined. Comparisons are made between optimized advanced composite structure and existing metal structure for those cases for which practical constraints include stiffnesses, strain levels, and manufacturing requirements.

INTRODUCTION

The commercial aircraft industry has had a history of producing new aircraft that offered improved efficiencies over preceding aircraft systems (Figure 1). The improved efficiencies have generally resulted from a series of major improvements in the propulsion system and configuration refinements. Comparatively speaking, improvements in structural weight have played only a minor role in producing improved economics.

Although no major breakthroughs in the area of structural weight have occurred, it has long been recognized that weight saving has a large potential for improving the economics of the commercial aircraft system. Using the DC-10-10 aircraft shown in Figure 2 as an example, it can be observed from Figure 3 that a 25-percent reduction of the secondary structure weight can reduce the total operating costs 1.5 percent and that a 25-percent reduction of the structural weight (primary and secondary) would result in a 7.5-percent reduction.

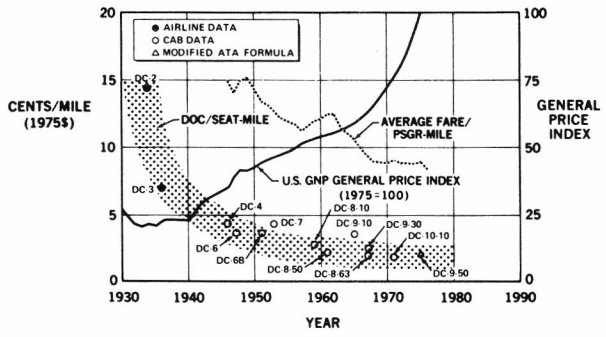

FIGURE 1. DIRECT OPERATING COST TRENDS

The recent development of advanced composite structures presents the potential for large reduction in transport structural weight in the 1985 to 1995 time period with the development of airframes utilizing composite structures. The advanced composites era was introduced in 1963 by the U.S. Air Force Project Forecast. Since that time there has been steady progress in the development of engineering methods, structural concepts, and

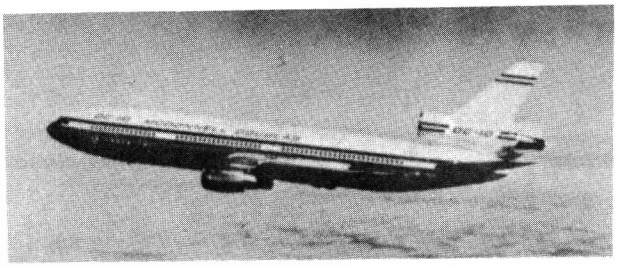

FIGURE 2. DC-10 SERIES 10 JET TRANSPORT

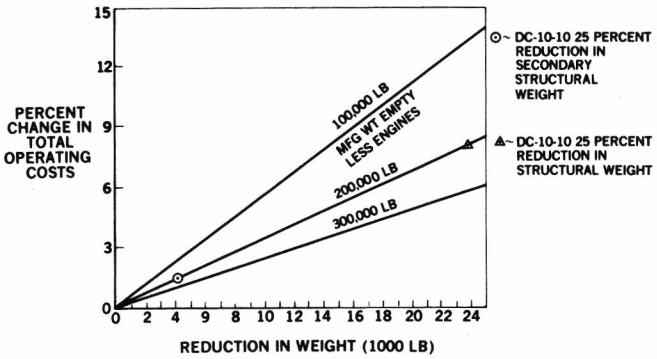

FIGURE 3. IMPACT OF WEIGHT REDUCTION ON TOTAL OPERATING COSTS

improved materials. Secondary structure components such as the DC-10 graphite/epoxy upper aft rudder shown in Figure 4 have been developed and placed in service.

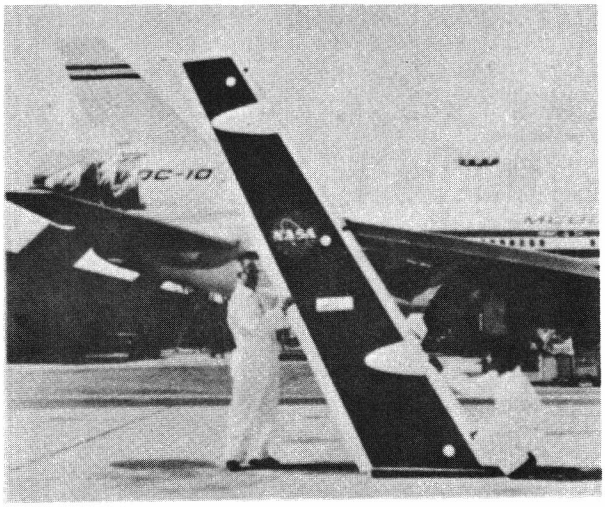

FIGURE 4. GRAPHITE/EPOXY RUDDER FOR DC-10-10

The high strengths and stiffnesses of the advanced composite materials provide the designer with the flexibility for a more weight-efficient solution to the vehicle strength and stiffness requirements. The objective of this paper is to discuss the newly developing area of composite structural element optimization and to demonstrate the potential impact of such techniques on the design of composite primary structures.

OPTIMIZATION OF COMPOSITE STRUCTURES

Although the discipline of optimization in structural design has become ever important in the past 10 years for conventional design, the advent of advanced composite materials in design has made this discipline even more important. In conventional design, the sizes and locations of fabricated parts are important in least-weight designs. With composite materials, not only are these factors still important, but a new dimension is added. The orientation in which the built-up plies are patterned is also vitally important to the weight of the structure. Hence, some sort of optimization is always incorporated in designs using the advanced composites.

Ply orientation is the most frequently encountered optimization problem in designing composite structures. Given a set of loading conditions, each consisting of combined membrane panel loads, and a set of minimum stiffnesses, what is the optimum pattern of ply orientations? In practice, it has been found that a reasonably good design can be determined if only 0-, ±45-, and 90-degree orientations are treated. In this case, it is only necessary to determine X = (L, M, N) from 3-dimensional design space, where L, M, and N denote the number of 0-, 90-, and ±45-degree plies, respectively. A series of computer programs and procedures for laminate optimization are discussed in Reference 1.

A method for selecting laminates of transport wing structures, optimized for both strength and flutter requirements, is presented in Reference 2. This technique takes advantage of the unique capability of composite structures to tailor independently the bending and torsional stiffnesses. The procedure starts with a search for the optimum pattern with no stiffness constraints. Stiffness and mass derivatives for the strength-only design are then used to obtain a minimum weight flutter-free design. Presented in Figure 5 is an application to a transport wing that

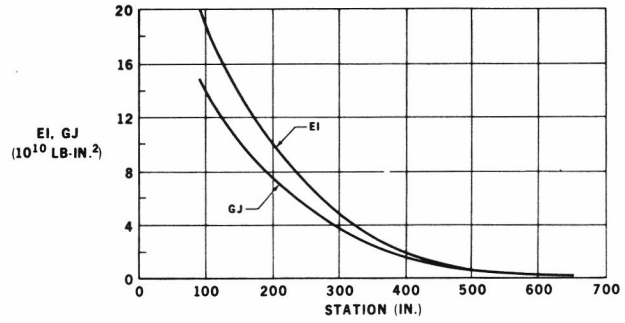

(a) METAL STIFFNESSES FOR STRENGTH AND STIFFNESS DESIGN

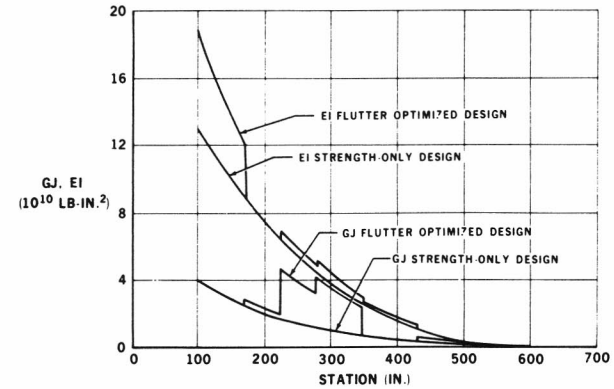

(b) COMPOSITE WING STIFFNESS DISTRIBUTION

FIGURE 5. COMPOSITE WING STRENGTH AND FLUTTER OPTIMIZATION

indicates the optimum stiffness distributions lie between the stiffnesses of the strength-only composite wing and the flutter-free metal wing.

A further development in the area of composite structures optimization is described in References 3, 4, and 5, where optimization procedures were used to size hat-, J-, and blade-stiffened compression panels. In Reference 4 the structural efficiency of graphite/epoxy and aluminum compression panels is compared as shown in Figure 6; in Reference 5 the structural efficiency of hat-, blade-, and J-stiffened panels are compared.

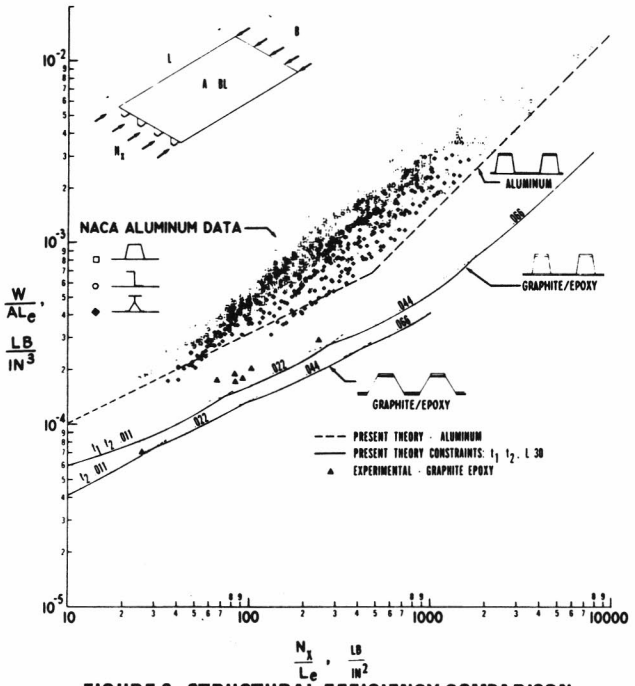

FIGURE 6. STRUCTURAL EFFICIENCY COMPARISON

STIFFENED PANEL OPTIMIZATION

In order to optimize stiffened compression panels and to study the impact of various constraints, a computer program was developed utilizing the analytical and optimization procedures described in Appendixes A and B. Two basic panel stiffening concepts emerged as the most promising from an initial screening of several candidate concepts shown in Figure 7. The preliminary screening of the candidates consisted of an efficiency evaluation of each of the concepts. Figure 8 shows the structural efficiency curves developed for panels with only strength constraints. The hat-stiffened panel was found to be the next-most efficient of the concepts considered and was selected for further evaluation. The second panel concept selected was the blade-stiffened panel. This concept, although the least efficient of the concepts considered, held the potential for low-cost fabrication.

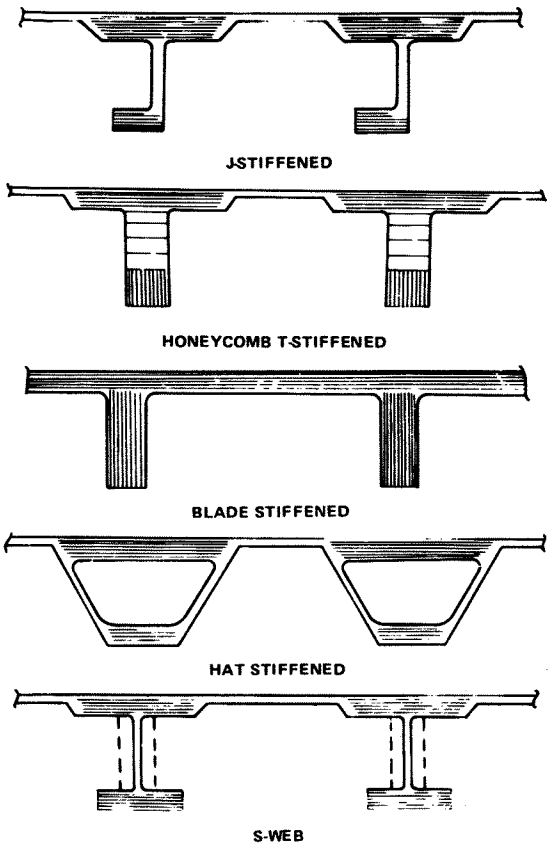

FIGURE 7. STIFFENED COMPOSITE COVER PANEL CONFIGURATION

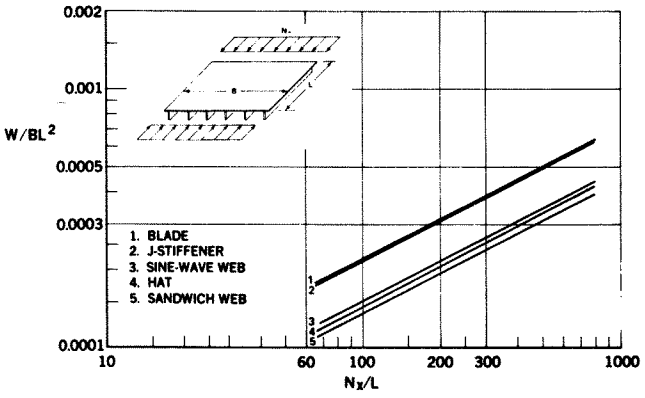

FIGURE 8. STRUCTURAL EFFICIENCY COMPARISON OF UNCONSTRAINED GRAPHITE DESIGN

The design variables of the two selected concepts, hat and blade stiffening, are illustrated in Figures 9 and 10. The basic optimization procedure provides for the design of these concepts with the listed design variables and with the potential for imposing various sets of stiffness and geometry constraints.

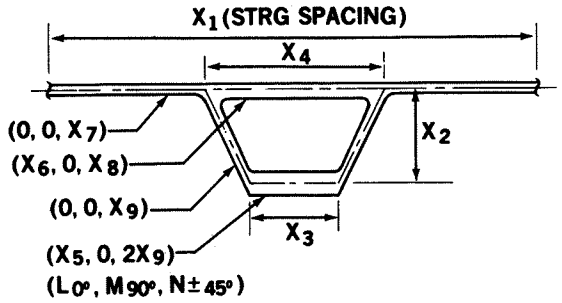

BASIC DESIGN CONSTRAINTS

$X_4 \leq X$
$X_3 < X$
$1/2\ t_p(X_5+X_6+X_8+2X_9) \leq X_2$
$0 \leq X_5$
$0 \leq X_6$
$0 \leq X_7$
$0 \leq X_8$
$0 \leq X_9$
$1/2\ t_p(X_5+2X_9)(X_4-X_3) \leq X_2X_3$

FIGURE 9. HAT STIFFENED PANEL DESIGN VARIABLES

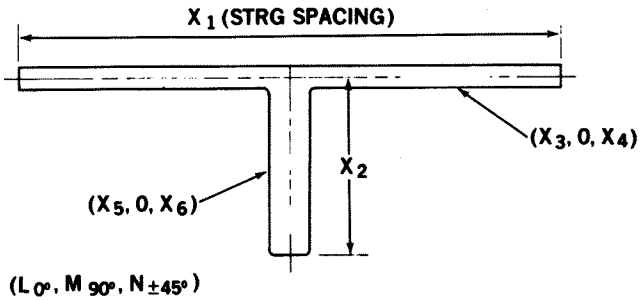

BASIC DESIGN CONSTRAINTS

$0 \leq X_3$
$4 \leq X_4$
$0 \leq X_5$
$4 \leq X_6$

FIGURE 10. BLADE STIFFENED PANEL DESIGN VARIABLES

OPTIMIZATION OF COMPOSITE TRANSPORT WING STRUCTURE

The stiffened panel optimization procedure was used to study the impact of various practical constraints on the upper wing covers of the DC-9-30, Figure 11. The aluminum covers have continuous skin from centerline to the tip assembly and are stiffened with Y-section stiffeners. The in-plane loads summarized in Figure 12 have maximum values of approximately 18,000 pounds per inch compression and 2900 pounds per inch shear.

The weights of composite panels which are unconstrained except by the load and area requirements of the wing can be determined by integrating the efficiency curves given in Figure 13. It should be noted, however, that there are a number of practical

FIGURE 11. DC-9 SERIES 30 JET TRANSPORT

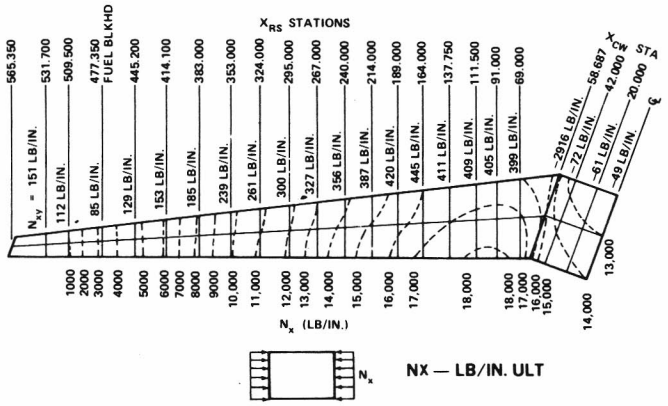

FIGURE 12. DC-9 UPPER SKIN PANEL LOADING

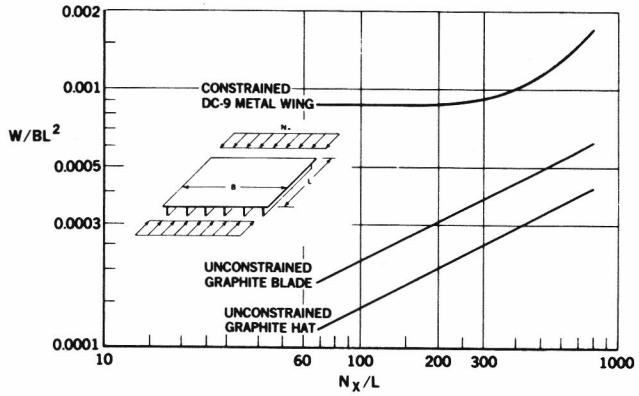

FIGURE 13. STRUCTURAL EFFICIENCY COMPARISON OF CONSTRAINED ALUMINUM DC-9 DESIGN WITH UNCONSTRAINED GRAPHITE DESIGN

constraints which the composite panels do not meet including practical fabrication constraints, minimum gauge requirements, out-of-plane loads, fail-safe requirements, and wing stiffness requirements.

One fabrication constraint is the requirement for constant stiffener spacing. In the totally unconstrained designs the stiffener spacing varied with load intensity. The effect on constant stiffener spacing is observed in Figure 14 where the efficiency curves are given for hat-stiffened panels which are restricted to spacings of 3 inches, 5 inches, and 7 inches and in Figure 15 where the efficiency curve for blades with 5-inch constant spacing is given.

A second set of constraints which has significant impact on the overall panel weight is the stiffness requirements. These stiffness levels result from minimum flutter and control reversal speed requirements and from related static and dynamic load criteria. The strength optimum blade- and hat-stiffened panels have much lower stiffnesses than the metal panel, Figures 16 and 17.

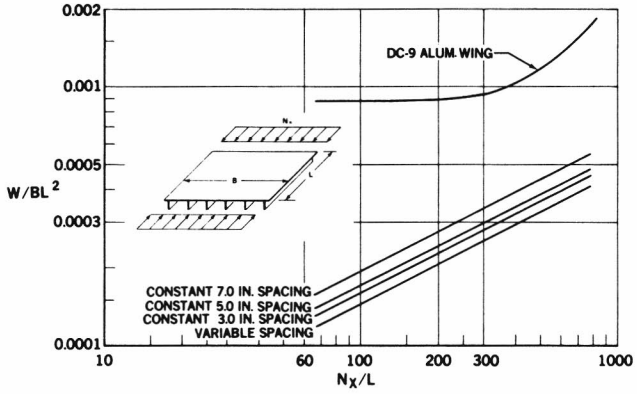

FIGURE 14. STRUCTURAL EFFICIENCY EFFECT OF CONSTANT STIFFENER SPACING ON UNCONSTRAINED GRAPHITE HATS

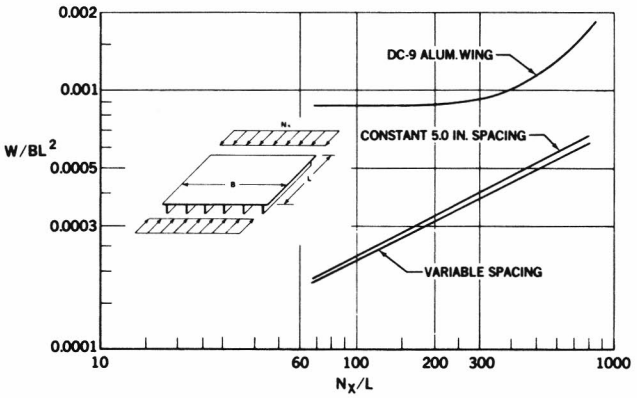

FIGURE 15. STRUCTURAL EFFICIENCY EFFECT OF CONSTANT STIFFENER SPACING ON UNCONSTRAINED GRAPHITE BLADES

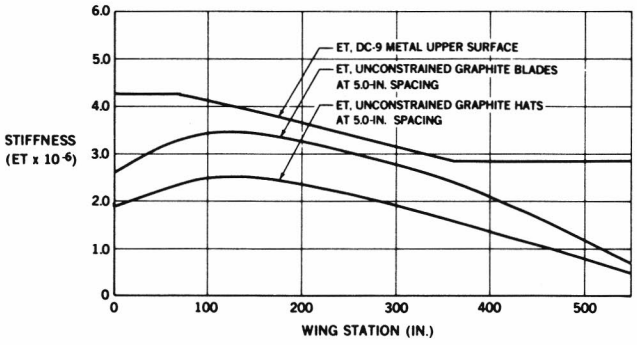

FIGURE 16. COMPARISON OF WING LONGITUDINAL STIFFNESSES

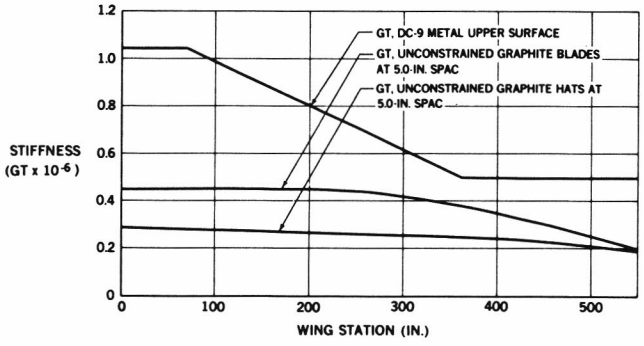

FIGURE 17. COMPARISON OF WING TORSIONAL STIFFNESSES

Restricting the hat- and blade-stiffened panels to the stiffnesses of the metal wing, the efficiencies given in Figure 18 are obtained. These designs were restrained to a constant 5-inch stiffener spacing. Section views of the unconstrained and stiffnesses constrained blade designs with 5-inch spacing at Station 300 are compared in Figure 19. These constraints dominate the designs to such a level that weight is not sensitive to the configuration. It can also be observed that weight is not particularly sensitive to stiffener spacing. Figure 20 shows the optimized weight of designs at Station 100 for increasing stiffener spacing.

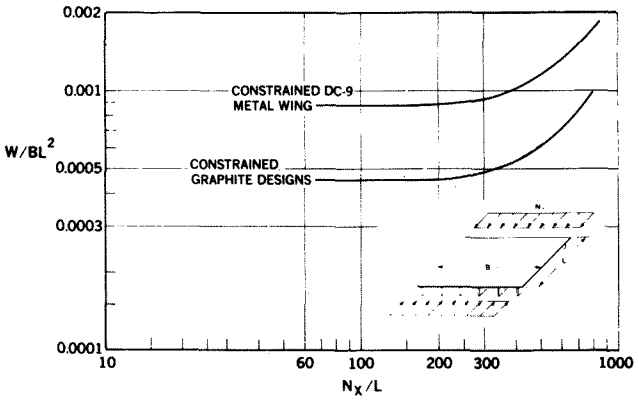

FIGURE 18. STRUCTURAL EFFICIENCY OF STIFFNESS CONSTRAINED GRAPHITE DESIGN

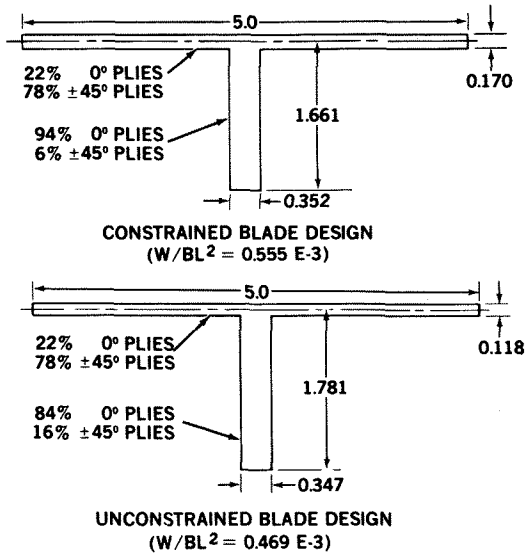

FIGURE 19. SECTION VIEW OF CONSTRAINED AND UNCONSTRAINED BLADE DESIGNS AT STATION 300 (N_x/L = 435)

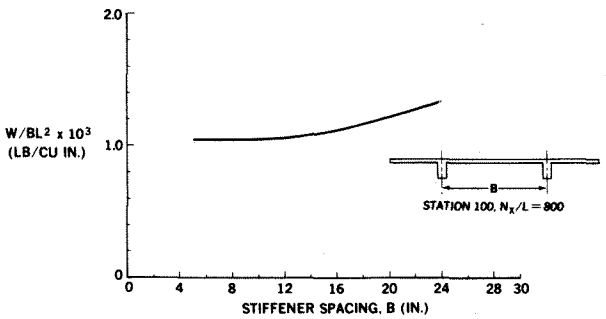

FIGURE 20. IMPACT OF INCREASED STIFFENER SPACING ON WEIGHT FOR CONSTRAINED DESIGNS

A further practical constraint that must be considered is that the wing cover panel has holes and the strains in the graphite/epoxy will have to be held below approximately 4000 inch per inch as an allowable strain level for laminates with small holes. Although in the hat-stiffened concept the holes could be placed in the all ±45-degree laminate area, the potential for misdrilled holes or subsequently drilled holes results in a similar constraint criterion. The change in the structural efficiency curve for the constrained hat- and blade-stiffened panels is presented in Figure 21.

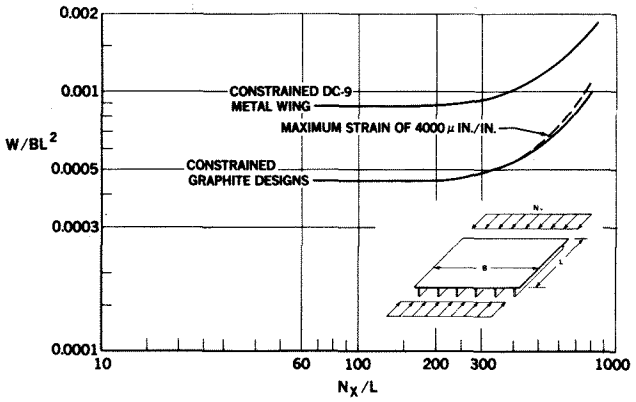

FIGURE 21. IMPACT ON STRUCTURAL EFFICIENCY FROM IMPOSING OF MAXIMUM STRAIN CONSTRAINT OF 4000 μ IN./IN.

Rib fixity was assumed to be simply supported for the cases studied. The specific value of the fixity will depend upon the method of attachment of the cover panel to the ribs. Several potential concepts for bolted clips are given in Figure 22. The specific value of the fixity is only a weight impact for the unconstrained designs. It should be noted, however, that although the weight does not change for the stiffness constrained designs, the configuration does change with fixity.

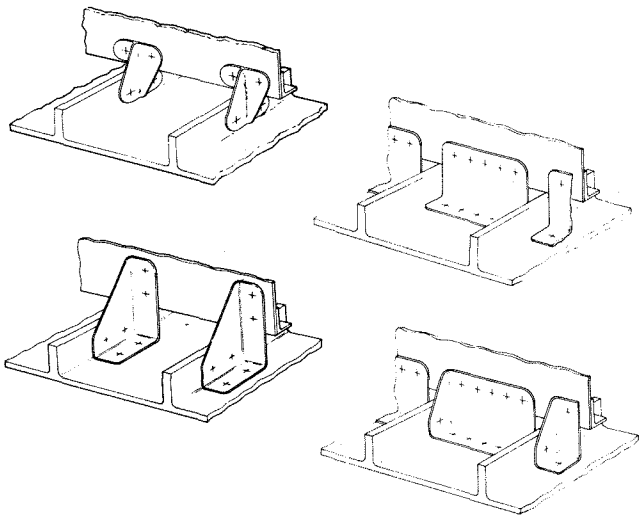

FIGURE 22. BOLTED CLIPS OF RIBS FOR BLADE STIFFENED PANELS

Although the weight comparisons have been made on the efficiency plots, the impact in terms of total weight saved is also of interest. Figure 23 compares the weight in pounds of the upper wing cover (both halves) for each of the concepts studied. It should be noted that the weight saving for the unconstrained designs is not obtainable in practice and is listed for reference only.

	UPPER COVER WEIGHT (POUNDS)	WEIGHT SAVING POTENTIAL
METAL BASELINE	2050	—
UNCONSTRAINED HAT STIFFENED	475	*
UNCONSTRAINED BLADE STIFFENED	725	*
STIFFNESS CONSTRAINED HAT AND BLADE STIFFENED	1115	46%
STIFFNESS CONSTRAINED PLUS 4000μ IN./IN. STRAIN MAXIMUM HAT AND BLADE STIFFENED	1160	43%

* DESIGNS HAVE INADEQUATE STIFFNESS

FIGURE 23. WEIGHT SAVING POTENTIAL

CONCLUSIONS

Stiffened panel optimization procedures have been shown to be a powerful tool for the design of composite structures. By changing the stiffener spacing during conventional practice, rib spacing or rib fixity has a major impact on the strength of a given design. When an optimization procedure is used, however, the configuration changes as the constraints change, but the weight and strength do not necessarily change significantly. This occurs in large transport aircraft structures because the stiffness constraints dominate the design and establish the minimum weight levels. The use of an optimization procedure, therefore, provides the opportunity to use a wide range of detailed configurations, stiffener spacings, rib attachments, and rib spacings that are consistent with the lowest-cost form of construction.

APPENDIX A
BUCKLING ANALYSIS OF BLADE-STIFFENED COMPRESSION PANELS

A buckling analysis of a blade-stiffened compression panel is derived, based on the simplifying assumption that the stiffener and skin modes are repeated for each stiffener bay. It is further assumed that the longitudinal deformations behave elastically and conform to plane strain theory. Finally, it is assumed that stiffener rotations occur about the intersection of the stiffener web and skin lines. A total of five modal coefficients are utilized in a Rayleigh-Ritz procedure, leading to an eigenvalue problem of dimension five. The five modal coefficients which are used to define the buckling mode of a single stiffener bay are illustrated and defined in Figure A-2.

The theory which is presented here is actually valid for a more general, J-shaped open-section stiffener, which of course, with a proper choice of configuration variables, reduces to a blade shape. The J-stiffened bay is broken down into the four components shown in Figure A-1.

① skin between stiffeners

② stiffener web

③ stiffener outer flange

④ stiffener attach flange plus skin

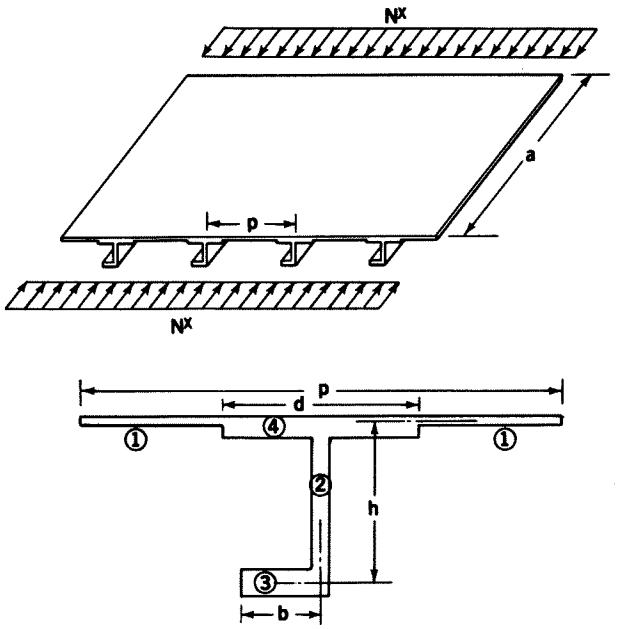

FIGURE A-1. J-STIFFENED COMPRESSION PANEL

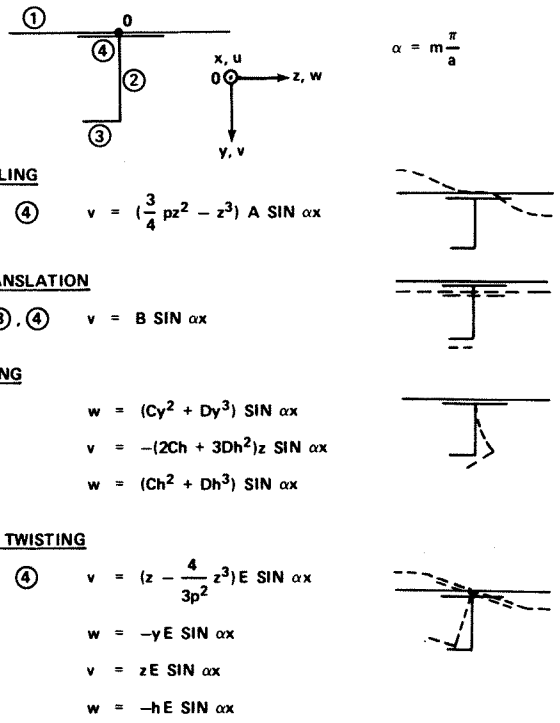

FIGURE A-2. ASSUMED BUCKLING MODE COMPONENTS

DISPLACEMENTS

Total displacements of the stiffener bay are defined in terms of the five modal coefficients as follows:

$$①\text{ and }④ \quad v = \left\{\left(\frac{3}{4}pz^2 - z^3\right)A + B + \left(z - \frac{4}{3p^2}z^3\right)E\right\}\sin\alpha x$$

$$w = 0$$

$$② \quad v = B\sin\alpha x$$

$$w = (Cy^2 + Dy^3 - Ey)\sin\alpha x$$

③ $v = (B - 2Chz - 3Dh^2z + Ez)\sin\alpha x$

$w = (Ch^2 + Dh^3 - Eh)\sin\alpha x$

LONGITUDINAL STRAINS

Commensurate with the usual assumptions of zero shear strains in open section torsional buckling problems, the longitudinal strains can be derived as follows:

② $\dfrac{\partial v}{\partial x} + \dfrac{\partial u}{\partial y} = 0$

$\dfrac{\partial u}{\partial y} = -\alpha B\cos\alpha x$

$u = -\alpha By\cos\alpha x + f(x)$

$\epsilon = \dfrac{\partial u}{\partial y} = \alpha^2 By\sin\alpha x + f'(x)$

③ $\dfrac{\partial w}{\partial x} + \dfrac{\partial u}{\partial z} = 0$

$\dfrac{\partial u}{\partial z} = \alpha(-Ch^2 - Dh^3 + Eh)\cos\alpha x$

$u = \alpha z(-Ch^2 - Dh^3 + Eh)\cos\alpha x + g(x)$

$\epsilon = \dfrac{\partial u}{\partial x} = \alpha^2 z(Ch^2 + Dh^3 - Eh)\sin\alpha x + g'(x)$

$\epsilon_{②} = \epsilon_{③}$ at $z = 0, y = h$

$\alpha^2 Bh\sin\alpha x + f'(x) = g'(x)$

$\epsilon_{①} = \epsilon_{②}$ at $z = 0, y = 0$

①and④ $\epsilon = f'(x)$

② $\epsilon = \alpha^2 By\sin\alpha x + f'(x)$

③ $\epsilon = \alpha^2 z(Ch^2 + Dh^3 - Eh)\sin\alpha x + \alpha^2 Bh\sin\alpha x + f'(x)$

In order to determine the unknown function, $f'(x)$, summation of longitudinal forces must be zero at every station.

$\int_A \epsilon EdA = 0$ Notationally, E appearing in EdA or Et terms denotes the elastic modulus.

$\therefore\ f'\int_A EdA + \sin\alpha x \int_{②} \alpha^2 ByEdA + \sin\alpha x \int_{③} [\alpha^2 z(Ch^2 + Dh^3 - Eh) + \alpha^2 BEh]\,EdA = 0$

$f' = (r_2B + r_3C + r_4D + r_5E)\sin\alpha x$

$Q = Et_{①}(p - d) + Et_{②}h + Et_{③}b + Et_{④}d$

$r_2 = -\dfrac{\alpha^2}{Q} Et_{②}\dfrac{h^2}{2} + Et_{③}bh$

$r_3 = \dfrac{\alpha^2 Et_{③}h^2b^2}{2Q}$

$r_4 = hr_3$

$r_5 = \dfrac{1}{h}r_3$

The longitudinal strains can finally be written

①and④ $\epsilon = (r_2B + r_3C + r_4D + r_5E)\sin\alpha x$

② $\epsilon = [(r_2 + \alpha^2 y)B + r_3C + r_4D + r_5E]\sin\alpha x$

③ $\epsilon = [(r_2 + \alpha^2 h)B + (r_3 + \alpha^2 h^2 z)C + (r_4 + \alpha^2 h^3 z)D + (r_5 - \alpha^2 hz)E]\sin\alpha x$

These strains can be further denoted as $\epsilon = \epsilon_o \sin\alpha x$

CURVATURE TERMS

①and④ $v_{,xx} = -\alpha^2\left[\left(\dfrac{3}{4}pz^2 - z^3\right)A + B + \left(z - \dfrac{4}{3p^2}z^3\right)E\right]\sin\alpha x$

$v_{,zz} = \left[\left(\dfrac{3}{2}p - 6z\right)A - \dfrac{8}{p^2}zE\right]\sin\alpha x$

$v_{,xz} = \alpha\left[\left(\dfrac{3}{2}pz + 3z^2\right)A + \left(1 - \dfrac{4}{p^2}z^2\right)E\right]\cos\alpha x$

② $w_{,xx} = -\alpha^2(Cy^2 + Dy^3 - Ey)\sin\alpha x$

$w_{,yy} = (2C + 6Dy)\sin\alpha x$

$w_{,xy} = \alpha(2Cy + 3Dy^2 - E)\cos\alpha x$

$v_{,xx} = -\alpha^2 B\sin\alpha x$

③ $v_{,xx} = -\alpha^2(B - 2Chz - 3Dh^2z + Ez)\sin\alpha x$

$v_{,zz} = 0$

$v_{,xz} = \alpha(-2Ch - 3Dh^2 + E)\cos\alpha x$

$w_{,xx} = -\alpha^2(Ch^2 + Dh^3 - Eh)\sin\alpha x$

STRAIN ENERGY

$U = \dfrac{1}{2}\int_0^a\int_{①}\epsilon^2 Et\,dzdx + \dfrac{1}{2}\int_0^a\int_{②}\epsilon^2 Et\,dydx$

$+ \dfrac{1}{2}\int_0^a\int_{③}\epsilon^2 Et\,dzdx + \dfrac{1}{2}\int_0^a\int_{④}\epsilon^2 Et\,dzdx$

$+ \dfrac{1}{2}\int_0^a\int_{①}(D_{11}v_{,xx}^2 + 2D_{12}v_{,xx}v_{,zz} + D_{22}v_{,zz}^2 + 4D_{66}v_{,xz}^2)\,dzdx$

$+ \dfrac{1}{2}\int_0^a\int_{②}(D_{11}w_{,xx}^2 + 2D_{12}w_{,xx}w_{,yy} + D_{22}w_{,yy}^2 + 4D_{66}w_{,xy}^2)\,dydx$

$$+\frac{1}{2}\int_0^a \int_{③} (D_{11}\, v_{,xx}^2 + 4D_{66}\, v_{,xz}^2)\, dzdx$$

$$+\frac{1}{2}\int_0^a \int_{④} (D_{11}\, v_{,xx}^2 + 2D_{12}\, v_{,xx} v_{,zz}$$

$$+D_{22}\, v_{,zz}^2 + 4D_{66}\, v_{,xz}^2)\, dzdx$$

The first four integrals represent the membrane strain energy, while the last four represent the bending strain energy. Integration over the length is separable and trivial since

$$\int_0^a \sin^2 \alpha x dx = \int_0^a \cos^2 \alpha x dx = \frac{a}{2}$$

Matrically, the strain energy can be written

$$U = \frac{a}{4} \begin{Bmatrix} A \\ B \\ C \\ D \\ E \end{Bmatrix}^T [Y] \begin{Bmatrix} A \\ B \\ C \\ D \\ E \end{Bmatrix}$$

where the elements of matrix Y are in terms of the geometric parameters only.

POTENTIAL ENERGY

$$W = \frac{\epsilon_{cr}}{2}\int_0^a \int_{①} v_{,xx}\, vEt\, dzdx$$

$$+\frac{\epsilon_{cr}}{2}\int_0^a \int_{②} (v_{,xx} v + w_{,xx} w)\, Et\, dydx$$

$$+\frac{\epsilon_{cr}}{2}\int_0^a \int_{③} (v_{,xx} + w_{,xx} w)\, Et\, dzdx$$

$$+\frac{\epsilon_{cr}}{2}\int_0^a \int_{④} v_{,xx} v\, Et\, dzdx$$

The potential energy is defined as the negative of the above work, W, of the external forces on the body, relative to the unstressed state (u = v = w = o). Here, the external forces can be visualized as fictitious forces arising from the longitudinal in-plane stresses rotating in conformity with the curvatures. The differential fictitious forces in the first integral can be expressed as

$$df = \sigma v_{,xx}\, dA\, dx = \epsilon_{cr} v_{,xx}\, Et\, dzdx$$

so that the differential work of the first integral is

$$dW = \frac{1}{2} v df = \frac{\epsilon_{cr}}{2} v_{,xx}\, v\, Et\, dzdx$$

Matrically, the work of the external forces can be written

$$W = \frac{a}{4} \begin{Bmatrix} A \\ B \\ C \\ D \\ E \end{Bmatrix}^T [Z] \begin{Bmatrix} A \\ B \\ C \\ D \\ E \end{Bmatrix}$$

THE EIGENVALUE PROBLEM

The eigenvalue problem is derived by applying the principle of the minimum of the total potential, which enforces the conditions of equilibrium. The total potential is

$$P = U - W = \frac{a}{4} X^T [Y - Z] X$$

where X now represents the vector $\{A\ B\ C\ D\ E\}$.

$$\frac{\partial P}{\partial X_i} = 0 \text{ for } i = 1, \ldots, 5$$

produces the eigenvalue problem $[Y - \epsilon_{cr} Z] X = 0$ and the minimum eigenvalue, ϵ_{cr}, is the buckling strain. A subroutine has been coded at Douglas for extracting the buckling strain from the above eigenvalue problem.

APPENDIX B
SEARCH ROUTINE FOR OPTIMIZATION

A computer program for searching for optimized structural configurations was coded in Fortran and is based on the method of feasible directions (Reference 6).*

In essence, a simplex problem is formulated and solved for the feasible search direction. To elaborate on this method, consider a configuration space which is divided between a feasible and an unfeasible portion, as illustrated by the simple, hypothetical, 2-dimensional problem shown in Figure B-1. The variables x_1 and x_2 represent dimensions of a structural configuration which are to be determined for an optimum design. In the case of composite laminate designs, the variables can also represent the number of plies in a particular orientation, or even the angle of the orientation itself. Although a 2-dimensional problem is the simplest that can be considered, it does lend itself to a visual understanding of the method. A constraint curve separates the feasible portion of the 2-dimensional configuration space from the unfeasible. In general, it consists of constraints imposed on the design variables, such as minimums and maximums, plus behavior variable constraints. Behavior variable constraints are: applied stress/allowable buckling stress = 1.0. Lines of constant weight are also shown in the figure. For the more general N-dimensional space, the constraints are hypersurfaces while the constant weight planes are hyperplanes.

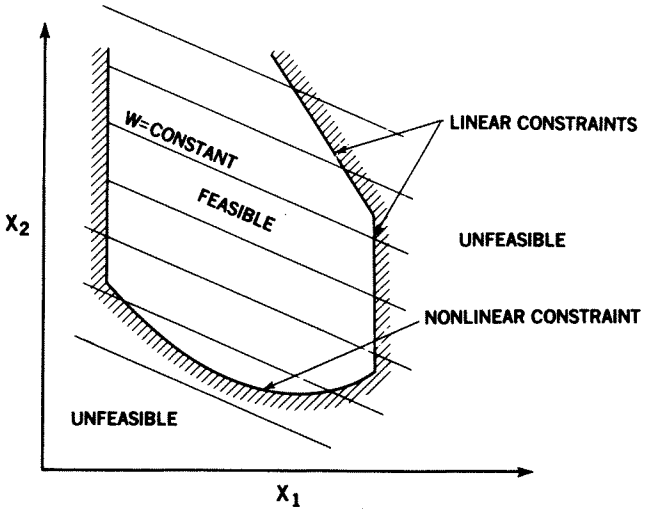

FIGURE B-1. HYPOTHETICAL CONFIGURATION SPACE

*For the convenience of the reader, the essential elements of this reference are reproduced here.

When the stepping process has reached a point on a general nonlinear constraint boundary, point B in Figure B-2, a new vector direction is carefully selected for an acceptable design improvement. To ensure that this vector direction be *feasible*, that is, not violate the constraint to within a linear approximation of the boundary at the point B, then the vector direction V must be related to the normal vector, P_x, by

$$\{V\}^T \{P_x\} \leq 0$$

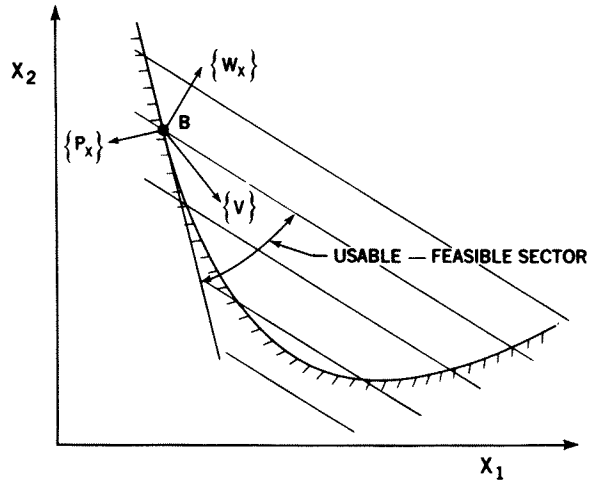

FIGURE B-2. DIRECTION FINDING PROBLEMS AT A CONSTRAINT

Defining the ratio of applied stress/allowable stress by P, which is a function of the configuration variables, x_i, the gradient vector $\{\partial P/\partial X_i\}$ can be computed at point B on the constraint surface. This vector is the normal to the constraint surface referred to above as P_x.

To ensure that this same direction be *usable*, that is, reduce the objective function, weight, the vector, V, must also be related to the weight gradient, W_x, by

$$\{V\}^T \{W_x\} \leq 0$$

These two conditions define the usable-feasible direction of search within the configuration space.

Any computational scheme that finds a direction of search within the bounds of these two inequalities can be referred to as a method of feasible directions. The particular scheme employed here is known as Zontendijk's method. It is based on solving a suboptimization problem for the direction vector. The added degree of complexity and computational effort is offset by a carefully selected search direction which, in the long run, reduces the number of gradient evaluations necessary.

Zontendijk's problem involves the maximization of a scalar, β, in accordance with the following conditions:

(1) $\{V\}^T \{P_x\} + \theta\beta \leq 0$

(2) $\{V\}^T \{W_x\} + \beta \leq 0$

(3) The length of $\{V\}$ is bounded.

The parameter, θ, is utilized as an adjustment to control the degree that the direction is biased by P_x. There is no bias for $\theta = 1$. For a linear constraint, the parameter θ should be set at $\theta = 0$, thus allowing the direction to be in the plane of the constraint. As the convex nonlinearity of the constraint increases, so too should θ, with the consequence of less weight reduction.

One way of satisfying condition (3) of Zontendijk's problem is to normalize the vector, V, by the criterion

$$|V_i| \leq 1 \qquad i = 1, \ldots, n$$

In order that the suboptimization problem be posed as a standard linear programming problem suited to a simplex solution, the transformation $V_i' = V_i + 1$ is made to ensure that V_i' remains positive. The final form of Zontendijk's problem becomes:

(a) $\{V'\}^T \{P_x\} + \theta\beta \leq \sum_{i=1}^{n} P_{x_i}$

(b) $\{V'\}^T \{W_x\} + \beta \leq \sum_{i=1}^{n} W_{x_i}$

(c) $0 \leq V_i' \leq 2 \qquad i = 1, \ldots, n$

This problem is now in the form:

maximize the scalar $Z = \{c\}^T x$

subject to the constraints $[A]\{x\} \leq \{b\}, \qquad x_i \leq 0$

which is recognized as the standard linear programming problem which is so suitably solved by the simplex algorithm.

Once the feasible direction is determined, a search is conducted along that direction until a constraint is encountered. A reduced weight is associated with this new design point. As this process is repeated, the search takes on a stepping appearance, bouncing between constraints as it approaches a converged design. This searching process is illustrated in Figure B-3. Of course, a number of programming type detail problems have been overcome in the course of the development of the computer program. Some of

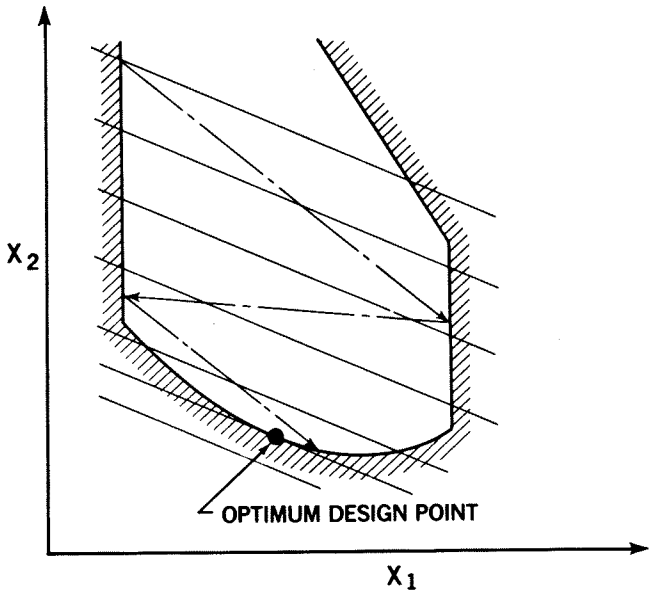

FIGURE B-3. SEARCH PROCESS FOR OPTIMIZED DESIGN

the improvements which have been incorporated into the searching process in an attempt to speed it up include:

- A transformation to consistent variables
- Retention of past constraint intercepts
- Recognition of "close" as well as "intercepted" constraints

REFERENCES

1. D. M. Purdy, "Composite Structures," International Symposium on Structural Mechanics Software, College Park, Maryland, June 1974.

2. D. M. Purdy, C. G. Dietz, and J. A. McGrew, "Optimization of Laminates for Strength and Flutter," Air Force Conference on Fibrous Composites in Flight Vehicle Design, Dayton, Ohio, September 1972.

3. J. G. Williams and M. M. Mikulas, Jr., "Analytical and Experimental Study of Structurally Efficient Composite Hat-Stiffened Panels Loaded in Axial Compression," AIAA Paper No. 75-754, presented at 16th Structures, Structural Dynamics, and Materials Conference, Denver, Colorado, May 1975 (also available as NASA TM X-72813).

4. M. M. Mikulas, Jr., H. G. Bush, and M. D. Rhodes, "Current Langley Research Center Studies on Buckling and Low-Velocity Impact of Composite Panels," 3rd Conference on Fibrous Composites – In Flight Vehicle Design, Williamsburg, Virginia, November 1975.

5. J. G. Williams and M. Stein, "Buckling Behavior and Structural Efficiency of Open-Section Stiffened Composite Compression Panels," AIAA/ASME/SAE 17th Structures, Structural Dynamics, and Materials Conference, Valley Forge, Pennsylvania, May 1976.

6. L. B. Gwin and S. C. McIntosh, Jr., "A Method of Minimum-Weight Synthesis for Flutter Requirements, Part I, Analytical Investigation," Technical Report AFFDL-TR-72-22 Part I, June 1972.